Research Square

Preprints are preliminary reports that have not undergone peer review.
They should not be considered conclusive, used to inform clinical practice,
or referenced by the media as validated information.

Synthesis and Properties of ionic liquid [ChIMIM][H2PO2] and its application in epoxy resin

Yiru Kong
Shenyang University of Chemical Technology
Yuanyuan Qiu
Shenyang University of Chemical Technology
Bing Liang
Shenyang University of Chemical Technology
Jiapeng Long
long2682@126.com
Shenyang University of Chemical Technology

Research Article

Keywords: Ionic liquid, Epoxy resin, Flame retardancy

Posted Date: November 20th, 2026

DOI: https://doi.org/10.21203/rs.3.rs-11336166/v1

License: This work is licensed under a Creative Commons Attribution 4.0 International License.
Read Full License

Additional Declarations: No competing interests reported.

Synthesis and Properties of ionic liquid [ChlMIM][H_2PO_2] and its application in epoxy resin

Yiru Kong[1], Yuanyuan Qiu[1], Bing Liang[1,*], Jiapeng Long[1,*]

[1] School of Material Science and Technology, Shenyang University of Chemical Technology, Shenyang 110142, People's Republic of China

Abstract

A novel phosphorus/nitrogen-containing ionic liquid Hypophosphite-type imidazolium ionic liquid ([ChlMIM][H_2PO_2]) was prepared by incorporating phosphorus-nitrogen compounds and applied in epoxy resin. The chemical structure of ([ChlMIM][H_2PO_2]) was confirmed by FTIR, ^{1}H NMR, and HRMS. The curing behavior, thermal stability, flame retardancy, combustion behavior, char structure, gaseous products, and mechanical properties of composite materials were investigated. At a phosphorus content of 0.21 wt.% (EP-4), the composite achieved an LOI value of 29.7% and a UL-94 V-0 rating. Compared with neat epoxy resin, its THR and PHRR decreased by 30.4% and 29.8%, respectively, while the char residue increased by 103.88%. SEM, Raman spectroscopy, and TG-IR analyses indicated that [ChlMIM][H_2PO_2] promoted the formation of a continuous and intumescent protective char layer and released nonflammable or flame-inhibiting species in the gas phase, revealing a condensed-phase/gas-phase synergistic flame-retardant mechanism. In addition, the tensile strength of EP-4 was 40.185 MPa, the impact strength and the flexural modulus were 4.5454 KJ/m^2 and 3150.4085 MPa.

Keywords: Ionic liquid; Epoxy resin; Flame retardancy

1. introduction

Epoxy resin (EP) is a representative thermosetting polymer widely used in electronic encapsulation, aerospace structures, rail transportation, coatings, adhesives,

Corresponding author 1: Jiapeng Long, Email: long2682@126.com
Corresponding author 2: Bing Liang, Email: lb1007@163.com

and high-performance composites because of its excellent adhesion, dimensional stability, chemical resistance, electrical insulation, and mechanical strength[1-6]. With the rapid development of advanced manufacturing and electronic/electrical industries, EP-based materials are required to provide not only structural reliability but also high fire safety[7-8]. However, conventional EP is intrinsically flammable because its aromatic and aliphatic structures readily decompose into combustible volatiles under heat or flame exposure, resulting in rapid ignition, high heat release, smoke release, and limited protective char formation[1-3]. These drawbacks restrict its use in engineering fields with strict fire-safety requirements. Therefore, it is highly important to develop efficient flame-retardant EP systems that can achieve high flame retardancy at low additive loading while maintaining mechanical performance. In this work, a structurally simple phosphorus/nitrogen-containing ionic liquid, [ChlMIM][H_2PO_2], was designed as a multifunctional additive to improve both fire safety and mechanical properties of EP.

Various strategies, including additive flame retardancy, reactive flame retardancy, and intrinsically flame-retardant molecular design, have been developed for EP[2,4-5]. Phosphorus-containing flame-retardants are among the most effective halogen-free systems because they can catalyze dehydration and carbonization in the condensed phase and quench active radicals in the gas phase[1,6,9]. Nitrogen-, silicon-, or sulfur-containing structures can further improve flame-retardant efficiency by diluting combustible gases, promoting intumescent char formation, and stabilizing the protective residue[9-13]. In addition, DOPO-based, bio-based, and hyperbranched flame-retardants have been reported to improve fire safety while partially preserving transparency, thermal resistance, and mechanical properties[14-17]. Despite these achievements, traditional additive flame-retardants usually require relatively high loadings, which may increase viscosity, reduce compatibility, cause aggregation, and deteriorate mechanical performance[5]. Reactive flame-retardants can reduce migration by entering the crosslinked network, but their synthesis is often complicated and their incorporation may alter curing behavior and crosslinking density[6]. Thus, balancing low loading, simple preparation, high flame-retardant efficiency, and mechanical

enhancement remains a key challenge.

Ionic liquids (ILs) have recently attracted attention in flame-retardant polymer design because of their tunable cation-anion structures, low volatility, relatively high thermal stability, and adjustable compatibility[18-20]. For EP systems, phosphorus-containing ILs are particularly promising because phosphorus and nitrogen elements can be integrated into one ionic structure, enabling condensed-phase and gas-phase synergistic flame-retardant effects. Previous studies have demonstrated that phosphorus-containing ILs, imidazolium phosphate ILs, DOPO-based ILs, and phosphorus-imidazole-based IL curing agents can improve LOI, UL-94 rating, heat-release behavior, toughness, and smoke suppression of EP composites[18,21-25]. Nevertheless, some reported IL flame-retardants still involve complex structures, multistep synthesis, or relatively high additive contents, and the relationship among curing behavior, char-layer formation, gaseous products, and mechanical properties has not been fully optimized. A simple phosphorus/nitrogen IL capable of improving flame retardancy and mechanical performance at low phosphorus content is therefore still desirable. As summarized in Table 1, although some reported systems exhibit a higher LOI or stronger heat-release suppression, the present system provides a more balanced combination of a V-0 rating, substantial reductions in THR and PHRR, and simultaneous tensile and impact enhancement at a low phosphorus content of 0.21 wt.%.

Table 1. Comparison of Properties of Different Flame-Retardant Epoxy Resin Systems

Ref.	FR system	Phosphorus content	LOI /UL-94	THR↓/PHRR↓ (%)	Tensile↑/Impact↑ (%)
[18]	TPP-PF6	2 wt.%	30.3 / V-0	45.81 / 36.32	— / —
[21]	DOPA-MZ	3 wt.%	30.3 / V-0	5.9 / —	22 / —
[22]	Imidazolium phosphate IL	1 wt.%	29.7 / V-0	—/—	≈10 / —
[25]	Liquid imidazole FR	15 wt.%	36.1 / V-0	37 / 70	— / —
This work	[ChlMIM][H_2PO_2]	0.21 wt.%	29.7 / V-0	30.4 / 29.8	≈13 / ≈5

In this study, a novel phosphorus/nitrogen-containing ionic liquid,

[ChlMIM][H_2PO_2], was synthesized and incorporated into the DDM-cured E-51 epoxy system. Its effects on curing behavior, thermal stability, fire safety, flame-retardant mechanism, and mechanical properties were systematically investigated. At a phosphorus content of only 0.21 wt.%, the optimized composite achieved an LOI of 29.7% and a UL-94 V-0 rating, while THR and PHRR decreased by 30.4% and 29.8%, respectively. The ionic liquid promoted protective char formation and gas-phase flame inhibition while improving mechanical performance, demonstrating its potential for low-phosphorus flame-retardant epoxy materials used in electronic encapsulation, coatings, adhesives, and structural composites.

2. Experimental

2.1 Experimental Materials

9,10-Dihydro-9-oxa-10-phosphaphenanthrene-10-oxide (DOPO), paraformaldehyde, chloroacetyl chloride, allyl glycidyl ether, 2-methylimidazole, phenylphosphoric acid, phenyldichlorophosphine and 1- (3-aminopropyl) imidazole were purchased from Shanghai McLin Biochemical Technology Co., Ltd. (Shanghai, China) Xylene, acetonitrile, dichloromethane and triethylamine were purchased from Sinopharm Group Chemical Reagents Co., Ltd. (Shanghai, China). All other reagents were used directly without further purification.

2.2 experimental preparation

2.2.1 Preparation of ionic liquid [ChlMIM] [H_2PO_2]

As shown in Fig.1, the synthetic route was described as follows. First, 18.01 g of pentaerythritol phosphate and 1.2 mL of triethylamine were added to a reaction flask and dissolved in 100 mL of acetonitrile. After complete dissolution of the mixture, 11.29 g of chloroacetyl chloride was slowly added dropwise. The mixture was mechanically stirred at 25 °C under an N_2 atmosphere for 6 h. After the reaction, acetonitrile was removed by vacuum distillation. The resulting white solid was collected by suction filtration after several washes with water, and the first-step product chloroacetylated pentaerythritol phosphate（PEPA-Chl） was obtained after vacuum

drying at 80 °C for 24 h.

Subsequently, 16.4 g of 2-methylimidazole, 14.2 g of acrylamide, and 2.4 mL of triethylamine were added to a reaction flask, dissolved in 120 mL of toluene, and mechanically stirred at 110 °C under an N_2 atmosphere for 24 h. After the reaction, toluene was removed by vacuum distillation. The product was washed several times with distilled water and filtered, and the second-step product acrylamide-modified methylimidazole （MIM） was obtained after vacuum drying at 100 °C for 24 h.

A total of 12.8 g of PEPA-Chl and 7.66 g of MIM were added to a three-necked flask equipped with a condenser and an exhaust-gas treatment device, dissolved in 100 mL of anhydrous ethanol, and mechanically stirred at 70 °C under an N_2 atmosphere for 24 h. After the reaction, anhydrous ethanol was removed by vacuum distillation to obtain a pale-yellow liquid product. The product chloride-type imidazolium ionic-liquid precursor ([ChlMIM]Cl) before ion exchange was obtained after vacuum drying at 80 °C for 24 h.

Finally, 19.7 g of [ChlMIM]Cl and 4.4 g of sodium hypophosphite were added to a reaction flask and dissolved in 100 mL of distilled water. The mixture was reacted at 80 °C for 24 h under mechanical stirring. After the reaction, distilled water was removed by vacuum distillation. The product and the by-product sodium chloride were transferred to anhydrous methanol and soaked for 4 h. Sodium chloride was removed by filtration, and anhydrous methanol was removed by vacuum distillation at 60 °C. The ionic liquid [ChlMIM][H_2PO_2] was finally obtained after vacuum drying at 80 °C for 24 h.

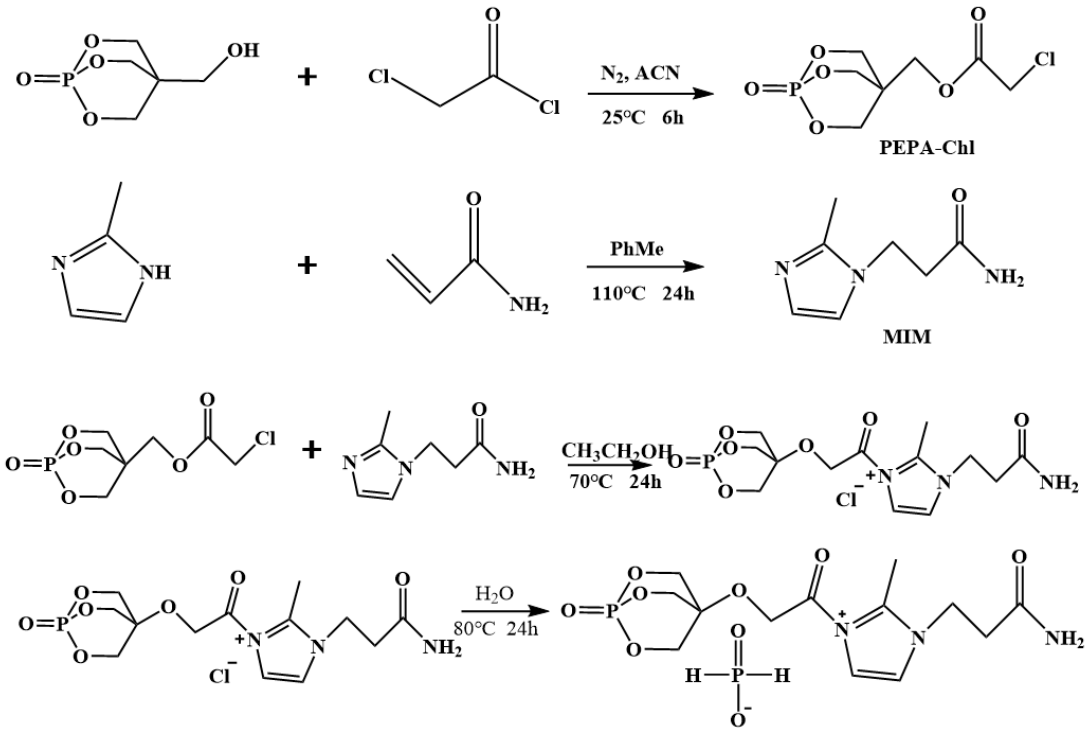


Fig.1 Synthesis route of [ChlMIM][H_2PO_2]

2.2.2 Preparation of [ChlMIM] [H_2PO_2]/DDM/EP composites

Bisphenol A epoxy resin (E-51) and ionic liquid [ChlMIM][H_2PO_2] were first blended at 60 °C and stirred to obtain a premix. The melted 4,4-diaminodiphenylmethane (DDM) curing agent was then added to the premix. After mechanical stirring and vacuum defoaming, the mixture was poured into molds and step-cured at 74 °C for 2 h, 112 °C for 4 h, and 160 °C for 2 h. After curing, the epoxy composite specimens were obtained by cooling and demolding. The detailed formulations are listed in Table 2.

Table 2 Experimental formulation of epoxy resin composites

Samples	E-51/g	Diluent/g	DDM/g	[ChlMIM][H_2PO_2]/g	P%(wt.%)
EP-0	100	10	25.28	0	0
EP-1	100	10	25.06	1	0.05
EP-2	100	10	24.60	3	0.11
EP-3	100	10	24.12	5	0.16
EP-4	100	10	23.66	7	0.21

2.3 Testing and characterization

Fourier transform infrared spectroscopy (FTIR): The chemical structure of [ChlMIM][H_2PO_2] was analyzed by the KBr pellet method using a Thermo Scientific Nexus-470 FTIR spectrometer (Thermo Fisher Scientific, USA). The spectral resolution was 1 cm^{-1}, and the scanning range was 400-4000 cm^{-1}.

Proton nuclear magnetic resonance spectroscopy (^1H NMR): The molecular structure of [ChlMIM][H_2PO_2] was characterized at room temperature using a Bruker 500 MHz NMR spectrometer (Bruker, Germany), with CD_4O as the solvent.

High-resolution mass spectrometry (HRMS): HRMS analysis was performed using an Agilent 6550 QTOF high-resolution mass spectrometer (Agilent Technologies, USA) equipped with an electrospray ionization (ESI) source. Methanol was used as the solvent, and spectra were recorded in positive-ion mode.

Curing behavior analysis: A NETZSCH DSC 3+ differential scanning calorimeter (NETZSCH Instruments GmbH, Germany) was used to investigate the curing behavior of the epoxy composites under nitrogen from 30 °C to 225 °C at heating rates of 2, 5, and 10 °C/min. The sample mass was approximately 5.0 mg.

Thermogravimetry (TG): A NETZSCH STA-449C simultaneous thermal analyzer (NETZSCH Instruments GmbH, Germany) was used to evaluate thermal stability. Approximately 10 mg of each sample was heated from room temperature to 800 °C at 20 °C/min under an N_2 atmosphere, with a sampling interval of 0.4 s.

UL-94 rating: A CZF-3 testing instrument (Nanjing Jiangning Instrument Factory, China) was used. The specimen dimensions were 130.0 × 9.5 × 4.0 mm^3, and the result for each group was averaged from five replicate specimens.

Limiting oxygen index (LOI): LOI measurements were conducted using a JF-3 apparatus (Nanjing Jiangning Instrument Factory, China). Each specimen was cut to 130.0 × 9.5 × 4.0 mm^3 in accordance with GB/T 2406-93. Five samples were tested per group, and the mass deviation was controlled within +/- 0.3 g. Limiting oxygen index is calculated according to Formula (1):

$$LOI = \frac{[O_2]}{[N_2]+[O_2]} \times 100\% \qquad (1)$$

Cone calorimeter test (CCT): An FTT 0007 cone calorimeter (Fire Testing Technology, UK) was used. According to ISO 5660-1, specimens with dimensions of 100.0 × 100.0 × 3.0 mm^3 were exposed to an external heat flux of 50 kW/m^2.

Thermogravimetry-infrared spectroscopy (TG-IR): A TGA Q50IR thermogravimetric analyzer (Bruker, Germany) coupled with a Nicolet 6700 infrared spectrometer was used. Approximately 5 mg of sample was placed in a crucible and heated from 30 °C to 800 °C under high-purity nitrogen.

Scanning electron microscopy (SEM): A JEOL JSM-6360 LV scanning electron microscope (JEOL Ltd., Japan) was used to observe the surface morphology of char residues after combustion. All specimens were sputter-coated with gold before observation.

Laser Raman spectroscopy: A LabRAM HR reflective confocal Raman spectrometer (HORIBA Scientific, France) was used to characterize the char residues after combustion.

Mechanical property analysis: Tensile tests were conducted according to GB/T 2567-2008 using a TCS-2000 microcomputer-controlled electronic universal testing machine (China Gaotie Technology Co., Ltd., China) at a tensile speed of 2 mm/min. The calculation formula for tensile strength (2) is as follows:

$$\sigma_t = \frac{P}{b \times h} \qquad (2)$$

Flexural tests were conducted according to GB/T 2567-2021 at a bending rate of 2 mm/min.

Impact strength was measured using a GT-704-MDL digital impact tester (China Gaotie Technology Co., Ltd., China) according to GB/T 2567-2021 with a simply supported beam setup and a 2 kJ pendulum hammer. Impact strength shall be calculated in accordance with Formula (3):

$$\sigma_k = \frac{A}{b \times d} \qquad (3)$$

3.Results and Discussion

3.1 FTIR Characterization of [ChlMIM][H_2PO_2]

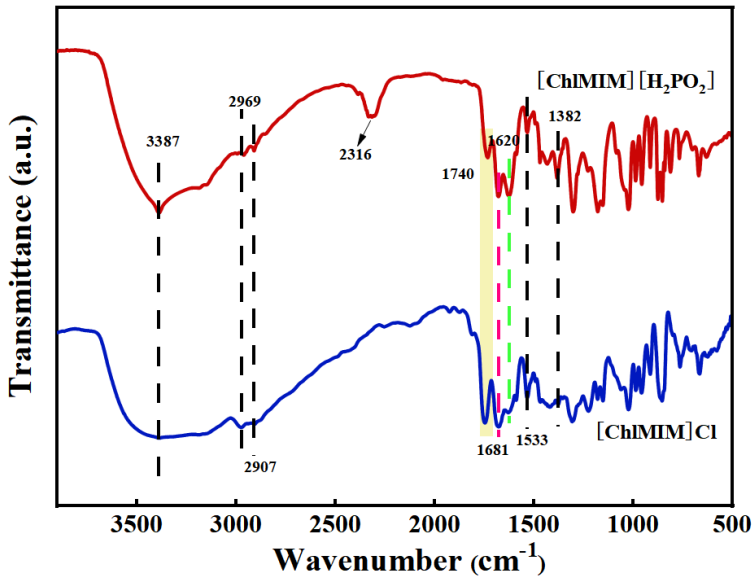


Fig. 2 FTIR spectrum of [ChlMIM][H_2PO_2]

Fig. 2 presents the FTIR spectra of [ChlMIM][H_2PO_2]. The peak at 1382 cm^{-1} corresponds to the characteristic bending vibration of saturated -CH bonds on methyl groups. The absorption peak at 1533 cm^{-1} is attributed to the stretching vibration of the imidazole skeleton. The peaks at 1620 cm^{-1}, 1681 cm^{-1} and 1740 cm^{-1} are ascribed to -NH_2 in-plane bending vibration, -C=O stretching vibration, and -P=O stretching vibration, respectively. The peaks at 2907 cm^{-1} and 2969 cm^{-1} originate from saturated -CH stretching vibrations of methyl and methylene groups, whereas the peak at 3387 cm^{-1} assigned to the -NH stretching vibration. The emergence of phosphite-related -PH stretching vibration peak at 2316 cm^{-1} verifies the successful ion exchange.

3.2 Analysis of ^{1}H NMR Spectra and Mass Spectrometry of [ChlMIM][H_2PO_2]

To confirm the successful preparation of the [ChlMIM][H_2PO_2], the chemical structure of [ChlMIM][H_2PO_2] was examined by NMR. The ^{1}H NMR spectrum in Fig. 3 a) contained the characteristic CD_4O solvent peak at δ = 3.35 ppm. The signal at δ = 2.64 ppm is assigned to the protons of the methylene (-CH_2). The peaks at δ = 2.85 ppm

and 3.85 ppm correspond to the protons of methyl groups and the hydrogen atoms on the methylene group attached to the imidazole skeleton, respectively. The signal at δ = 4.47 ppm originates from the protons of the methylene group connected to O=P-O (the electron-withdrawing inductive effect of the -P=O bond shifts the chemical shift of methylene hydrogens downfield, i.e., increases the δ value). The signal at δ = 4.70 ppm is ascribed to the protons of the methylene group bonded to the -C=O bond. The signal at δ = 4.85 ppm is attributed to the hydrogen atom of the P-H bond on the hypophosphite anion. The signals at δ = 6.51 ppm and 7.80 ppm correspond to amino hydrogens (-NH_2) and the hydrogen atoms on the imidazole skeleton (-CH=CH), respectively. The NMR assignments confirmed that the precursor structure was fully consistent with the theoretical structure of [ChlMIM][H_2PO_2].

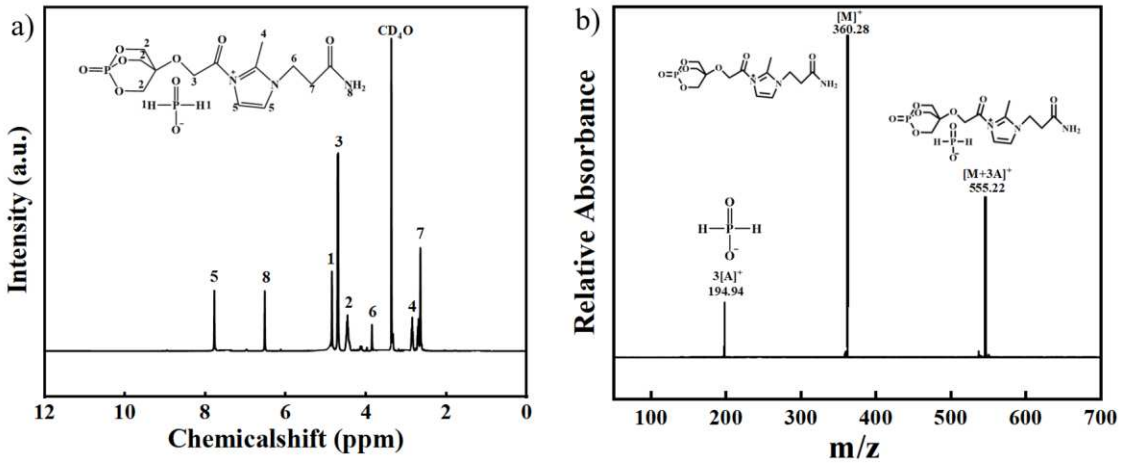


Fig.3 ^{1}H NMR spectrum (a) and mass spectrum (b) of [ChlMIM][H_2PO_2]

Table 2 Mass-to-charge ratios of different fragments

mass spectrum fragments	$[3A]^+$	$[M]^+$	$[M+3A]^+$
Molecular weight	194.94	360.28	555.22

The mass spectra of [ChlMIM][H_2PO_2] are presented in Fig. 3 b) and Table 2. The peaks at m/z = 194.94, 360.28 and 555.22 correspond to $[3A]^+$, $[M]^+$ and $[M+3A]^+$ respectively, where M denotes the cationic of [ChlMIM][H_2PO_2] and A represents the anionic structure of [ChlMIM][H_2PO_2]. The mass spectrometry results are in good agreement with the theoretical molecular weight of [ChlMIM][H_2PO_2].

Combined with the FTIR, ^{1}H NMR and mass spectrometry analyses of [ChlMIM][H_2PO_2], the structure of the as-synthesized [ChlMIM][H_2PO_2] matches the

designed molecular structure. These results confirm the successful synthesis of the ionic liquid [ChlMIM][H_2PO_2].

3.3 Thermal analysis of [ChlMIM][H_2PO_2]/DDM/EP System

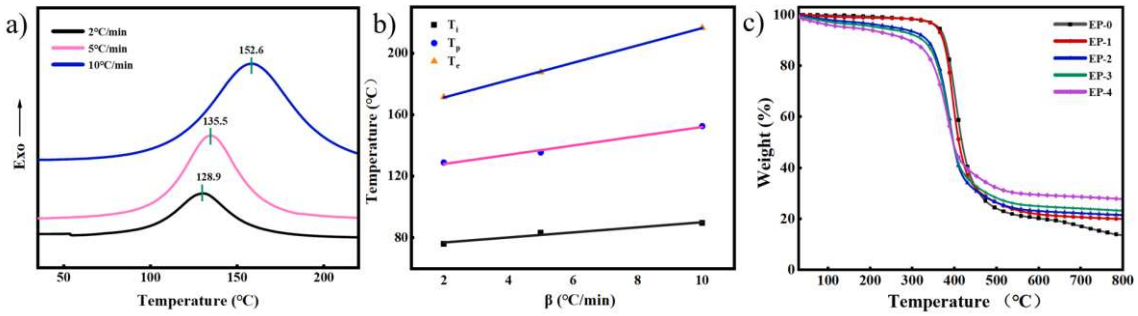


Fig. 4 Thermal analysis of [ChlMIM][H_2PO_2]/DDM/EP system: a) DSC curves at different heating rates; b) relationship between heating rate and characteristic temperatures; c) TG curves of EP composites with different formulations.

Differential scanning calorimetry (DSC) was employed to investigate the the curing reaction of [ChlMIM][H_2PO_2]/DDM/EP composite system. Non-isothermal DSC tests for the curing reaction were performed at three heating rates of 2 °C/min, 5 °C/min and 10 °C/min. As shown in Fig. 4a), the exothermic peak positions of the curing reaction vary with heating rates, and the curing reaction exothermic peak gradually shifts to higher temperature as the heating rate increases[2]. To obtain the characteristic curing temperatures of the composite, peak and end the temperatures of the exothermic peaks were extracted from non-isothermal DSC curves and denoted as T_i, T_p and T_e, where β stands for the heating rate. Plots of T_i, T_p and T_e against heating rate β are shown in Fig. 4b). The gelation temperature, curing temperature and post-treatment temperature can be obtained by extrapolating the fitted straight lines to $\beta = 0$. Based on the DSC data results, the curing process of the composite material was determined as follows: curing at 74 °C for 2 h, followed by curing at 112 °C for 4 h, and finally curing at 160 °C for 2 h.

The thermogravimetric curves of epoxy resin composites are shown in Fig. 4c). The epoxy resin composites filled with [ChlMIM][H_2PO_2] (EP-1 to EP-4) undergo the same thermal degradation process as neat epoxy resin (EP-0). At the first stage where

the temperature is below 300 °C, the mass loss of samples mainly arises from water volatilization, and the variation in sample mass loss is insignificant. The second stage occurs at 300-500 °C, during which the samples suffer rapid mass loss caused by the backbone cleavage of epoxy macromolecules. In the final stage, the mass variation of the composites levels off. Nevertheless, the carbon residue of the composites changed significantly upon incorporating [ChlMIM][H_2PO_2]. A higher char yield indicates superior flame retardancy of epoxy resin composites, as it generally corresponds to a denser char layer formed during combustion and serves as a critical indicator for evaluating the condensed-phase flame-retardant mechanism[1]. The carbon residue of EP-0 was merely 13.65%. By contrast, The carbon residue of EP-4 was 27.83%, which was a 103.88% increase compared to EP-0. This fully demonstrates that [ChlMIM][H_2PO_2] remarkably enhances the flame-retardant performance of epoxy resin composites.

3.4 Flame Retardancy Analysis of [ChlMIM][H_2PO_2]/DDM/EP System

the flame retardancy of epoxy resin composites was evaluated via limiting oxygen index (LOI) and UL-94 vertical burning tests. The LOI is defined as the minimum volume fraction of oxygen in an oxygen-nitrogen mixture required to sustain combustion of specimen, serving as a standard indicator for characterizing material flammability. A higher LOI value indicates that the material is less prone to combustion in air. Table 4 present the LOI and UL-94 test results of [ChlMIM][H_2PO_2]/DDM/EP composites. The neat epoxy resin (EP-0) only exhibited an LOI value of only 22.9%, classifying it as a flammable material with no UL-94 flame-retardant rating. With increasing flame-retardant increasing loading from EP-1 to EP-4, the LOI value rises from 25.5% to 29.7%, indicating steady improvement in the flame-retardant performance. The flame-retardant rating upgrades from V-1 for EP-1 and EP-2 to V-0 for EP-3 and EP-4, meeting a superior flame-retardant standard.

Furthermore, the self-extinguishing times after two ignitions (t_1 and t_2) decreased significantly drastically shortened with rising flame-retardant content. For EP-4, t_1 is merely 5.5 s and t_2 is only 4.6 s, demonstrating that the flame-retardant can effectively

suppresses flame spread and enable rapid self-extinguishment of the material. This phenomenon occurs because the introduction of [ChlMIM][H_2PO_2] introduces phosphorus and nitrogen elements that facilitate char formation in the composite and greatly improve the quality of the char layer. The resulting char layer effectively hinders the further combustion of epoxy resin and isolates the combustion zone from flammable gases.

Table 4 LOI and UL-94 vertical burning results of samples with different compositions

Samples	LOI(%)	UL-94	t_1(s)	t_2(s)	Dripping
EP-0	22.9	——	> 30	——	Yes
EP-1	25.5	V-1	15.9	14.7	No
EP-2	27.4	V-1	12.0	11.5	No
EP-3	28.8	V-0	8.5	7.2	No
EP-4	29.7	V-0	5.5	4.6	No

The flame-retardant performance of the composite materials was further investigated via cone calorimetry. Cone calorimetry provides critical reference for material evaluation, formulation design and fire prevention. In cone calorimetry tests, the heat release rate curve and total heat release curve serve as core curves for assessing the combustion behavior of materials. These two curves jointly reflect the fire hazard of materials from the perspectives of heat release intensity and cumulative total heat release. Fig. 5 a) and b) display the total heat release curve and heat release rate curve of the [ChlMIM][H_2PO_2]/DDM/EP composite material, respectively. Incorporation of [ChlMIM][H_2PO_2] drastically reduces the THR and PHRR of EP composites. Compared with neat EP-0, the THR and PHRR of EP-4 decrease by 30.4% and 29.8% respectively. This result further confirms that the incorporation of [ChlMIM][H_2PO_2] effectively enhances the flame-retardant performance of composites. As shown in Fig. 6, the flame-retardant effect of [ChlMIM][H_2PO_2] follows a typical intumescent flame retardant mechanism, which consists of three components: acid source, carbon source and gas source. Upon heating, phosphorus-containing groups decompose to produce H_3PO_4 or polyphosphate substances acting as the acid source, which catalyze the dehydration, crosslinking and carbonization of the epoxy resin matrix. The epoxy resin

and organic groups in [ChlMIM][H_2PO_2] serve as the carbon source to form a continuous char layer; nitrogen-containing structures release non-flammable gases such as NH_3 and N_2, which act as the gas source to expand the softened char layer and dilute combustible volatiles. A dense intumescent char layer is ultimately formed to effectively block the transfer of heat, oxygen and combustible decomposition products. Meanwhile, phosphorus-containing substances can capture active hydrogen radicals (H·) and hydroxyl radicals (·OH) in the gas phase, further interrupting the combustion chain reaction. In summary, the improved flame retardancy of epoxy resin composites originates from the synergistic effect of condensed-phase char formation, gas-phase dilution and radical scavenging.

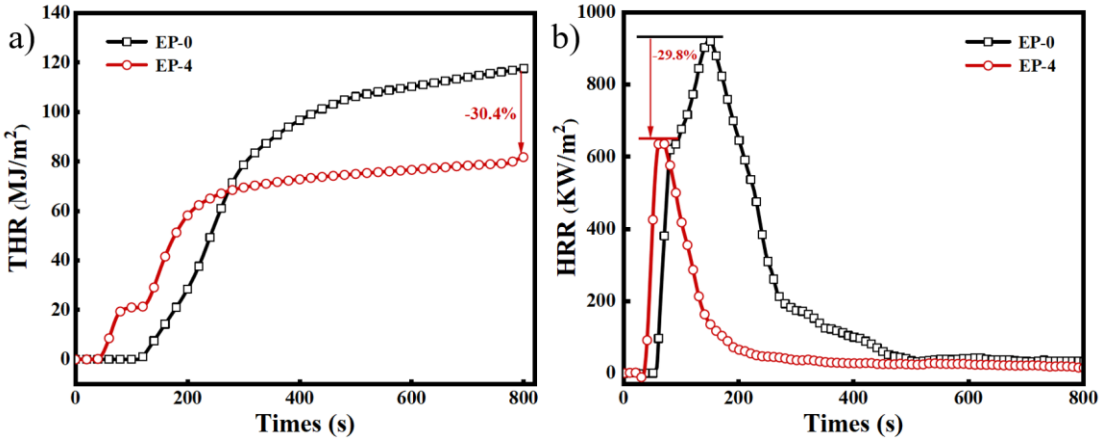


Fig. 5 Cone calorimetric test analysis a) THR curves of [ChlMIM][H_2PO_2]/DDM/EP composites b) HRR curves of [ChlMIM][H_2PO_2]/DDM/EP composites

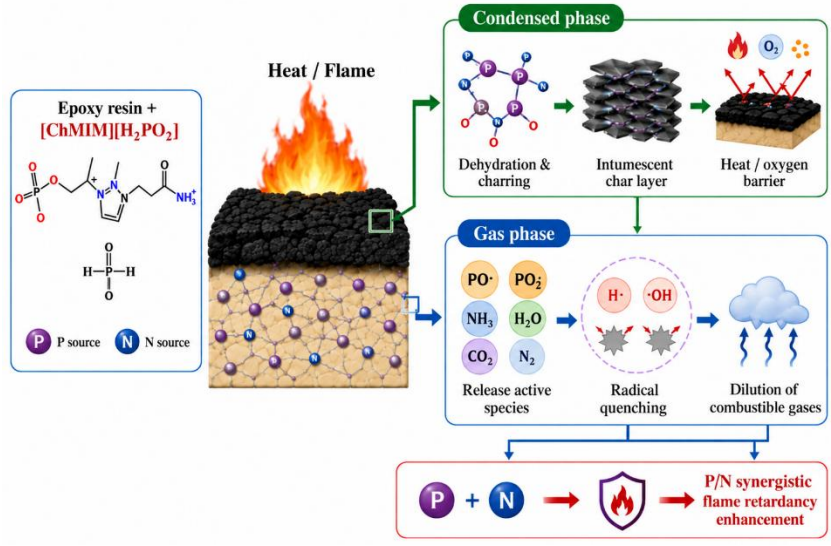


Fig. 6 Flame-retardant mechanism of [ChlMlM][H_2PO_2] in epoxy resin

3.5 SEM Characterization of Residue Carbon from [ChlMIM][H_2PO_2]/DDM/EP System

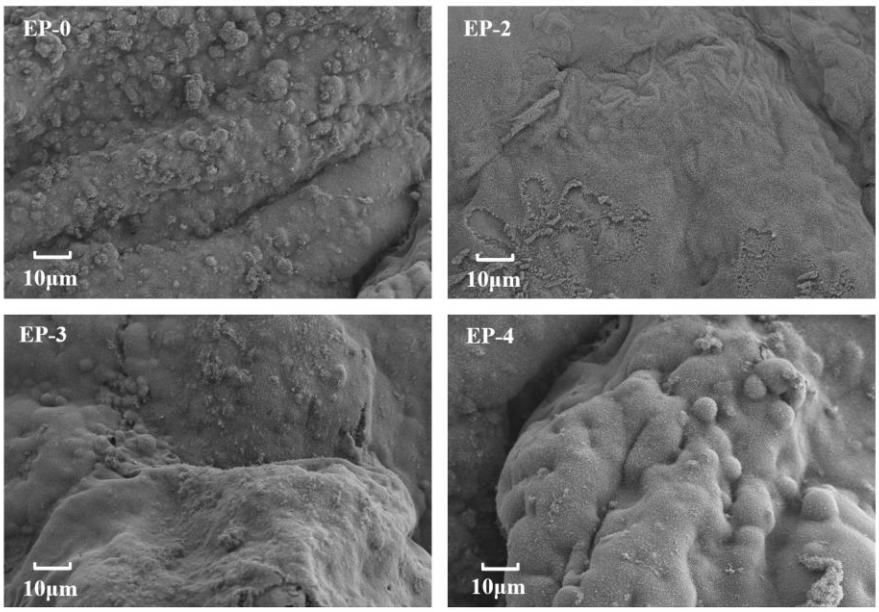


Fig. 7 SEM images of [ChlMIM][H_2PO_2]/DDM/EP composites

Scanning electron microscopy (SEM) morphologies of residual char of EP-0, EP-2, EP-3 and EP-4 composites are shown in the Fig. 7. It can be observed from the images that the surface of EP-0 exhibits a typical rough and porous structure, which is formed by the disorderly accumulation of numerous loose particles, presenting overall surface irregularity and remarkable porosity. After incorporating [ChlMIM][H_2PO_2], the surface morphology of EP-2 undergoes dramatic changes, with drastically reduced roughness, a smoother surface and a more continuous overall structure.

With further increase in flame-retardant loading, the evolutionary trend of surface morphology of EP-3 and EP-4 residual char becomes more evident. Dispersed spherical-like protrusions start to emerge on the surface of EP-3; these protrusions are unevenly distributed and relatively small in size. For EP-4, both the number and size of the sphere-like protrusions rises significantly with a marked increase in size, and the agglomeration or spheroidization phenomenon on the surface becomes more prominent. The overall morphology gradually transforms from the initial loose porous structure to an aggregated structure dominated by spherical particles.

This morphological evolution is associated to the phosphorus-and-nitrogen

containing moieties in the structure of [ChlMIM][H_2PO_2]. During pyrolysis, the phosphorus-containing species catalyze the dehydration, cross-linking and other reactions of epoxy resin. The formed phosphorus-containing cross-linked network can strengthen the char layer, preventing it from cracking under the impact of heat flow or gas flow and maintaining the integrity of the protective barrier. Moreover, this barrier can effectively isolate heat and oxygen and restrain the escape of combustible volatile components[1-9]. Nitrogen elements decompose and release non-combustible gases upon heating, which can expand the softened char layer to form an intumescent char layer with closed-cell structures[9]. This mechanism accounts for the appearance of spherical protrusions on EP-3 and EP-4.

3.6 Raman Spectral Characterization of Residue Carbon from [ChlMIM][H_2PO_2]/DDM/EP System

Raman spectroscopy is a classic method for analyzing the disorder degree and graphitization degree of carbon materials, which generally focuses on the intensity ratio (ID/IG value) of the D band (~1350 cm^{-1}, representing defective and disordered carbon) and the G band (~1580 cm^{-1}, representing the in-plane vibration of sp^2-hybridized carbon in graphite lattices). A lower ID/IG ratio of residual char indicates a higher degree of graphitization, corresponding to the formation of more continuous and stable graphite-like protective layers.

Fig. 8 is Raman spectra of the [ChlMIM][H_2PO_2]/DDM/EP composites. The ID/IG ratio of residual carbon in the pure epoxy resin EP-0 sample is 0.89, while that of the EP-4 sample incorporated with [ChlMIM][H_2PO_2] is 0.78. This demonstrates that [ChlMIM][H_2PO_2] facilitates the formation of a more ordered and continuous carbon layer in EP samples. During densification, the carbon structures partial ordered rearrangement, which moderately increase the size of graphite microcrystals, optimizes their arrangement and reduce internal defects. The enhanced orderliness of internal carbon structures accounts for the transformation of macroscopic morphology from loose to compact. The improved internal structural ordering arises from the large-scale catalytic formation of aromatic cross-linking networks by [ChlMIM][H_2PO_2] in the

early initial pyrolysis stage, which rapidly immobilize carbon skeletons and inhibits disordered cracking, ulitimately producing a denser, smoother char layer with reduced defects lower ID/IG ratio[1].

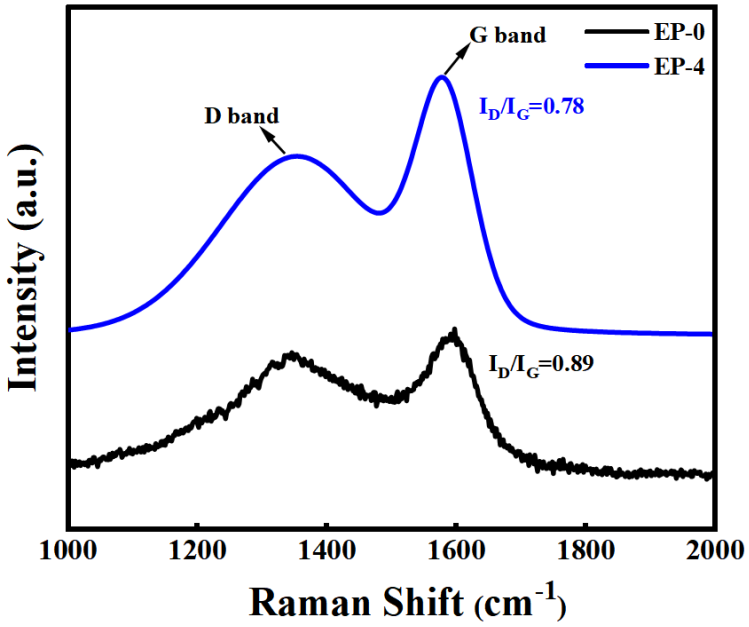


Fig. 8 Raman spectra of the [ChlMIM][H_2PO_2]/DDM/EP composites

3.7 TG-IR Characterization of [ChlMIM][H_2PO_2]/DDM/EP System

Fig. 9 a) and b) present the TG and DTG curves of EP-0 and EP-4, respectively. EP-0 undergoes a rapid mass loss around 400 °C, and the peak mass loss rate on its DTG curve is sharp, indicating concentrated and intense thermal decomposition. In contrast, EP-4 containing [ChlMIM][H_2PO_2] exhibited only a slight change in T_{max} (the temperature at the maximum mass loss rate), yet its DTG curve showed a gentler mass loss peak and a markedly higher char yield at 800 °C. This reveals that P-N synergism facilitates char formation in the composite material, and the char layer restrains the continuous decomposition of the material[1-9].

Fig. 9 c) and d) present the infrared spectra corresponding to EP-0 and EP-4. At low heating temperatures (approximately 100-300 °C), the P-N bonds in the structure of [ChlMIM][H_2PO_2] cleave first, which effectively accelerates the cross-linking and char-forming reactions of benzene rings in EP-4 and thereby suppresses the thermal decomposition of aromatic rings at elevated temperatures. For this reason, the infrared

characteristic peaks of C-H bonds cannot be detected in EP-4 under high-temperature conditions. As the temperature further rises to roughly 400-500 °C, phosphorus-containing groups thermally convert into polyphosphoric acid, accompanied by the emergence of a characteristic peak of P=O bonds at 1218 cm^{-1}, which verifies the formation of polyphosphoric acid structures. Polyphosphoric acid effectively scavenges H· and ·OH radicals in the gas phase, thereby inhibiting chain reactions. Temperatures of approximately 400-600 °C induced the decomposition of nitrogen-containing species, releasing ammonia with a characteristic absorption at 812 cm^{-1}. NH_3 can dilute the concentration of CO_2 in the gas phase[9]. Meanwhile, polyphosphoric acid converted from phosphorus-containing groups further inhibits the generation of H_2O and CO_2 by capturing free radicals.

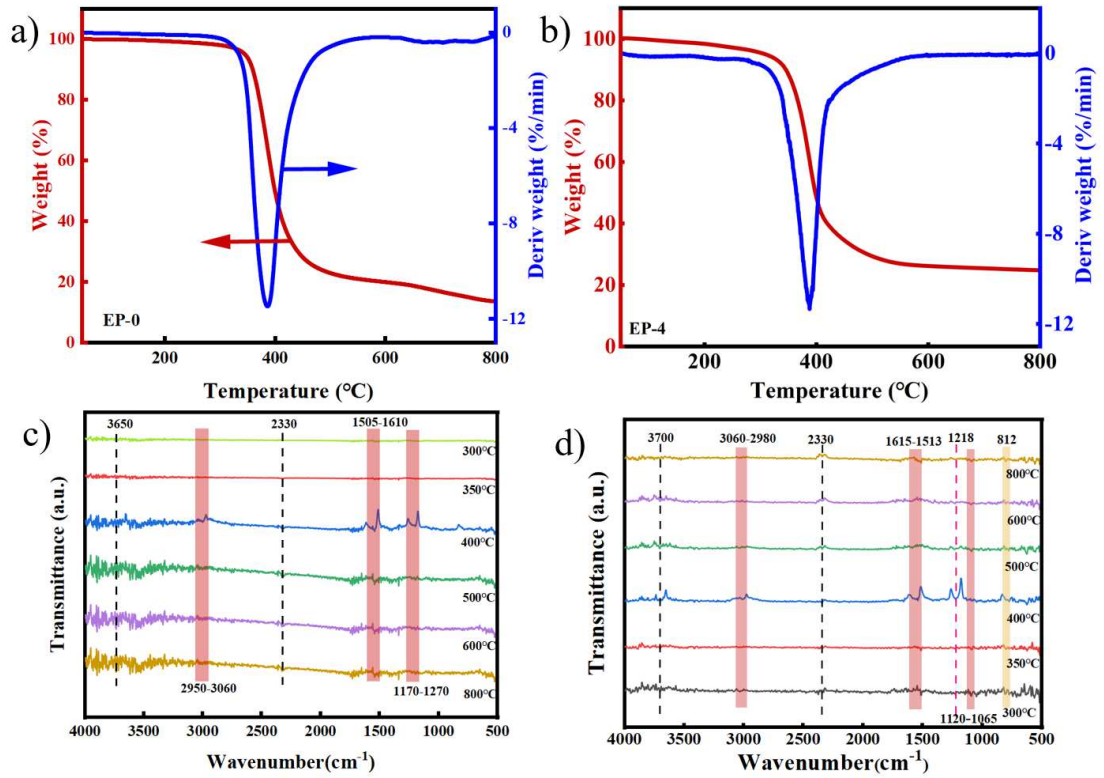


Fig. 9 Results of TG-IR a) EP-0 TG curve b) EP-4 TG curve. c) EP-0 FT-IR spectra d) EP-4 FT-IR spectra

3.8 Study on Mechanical Properties of [ChlMIM][H_2PO_2]/DDM/EP System

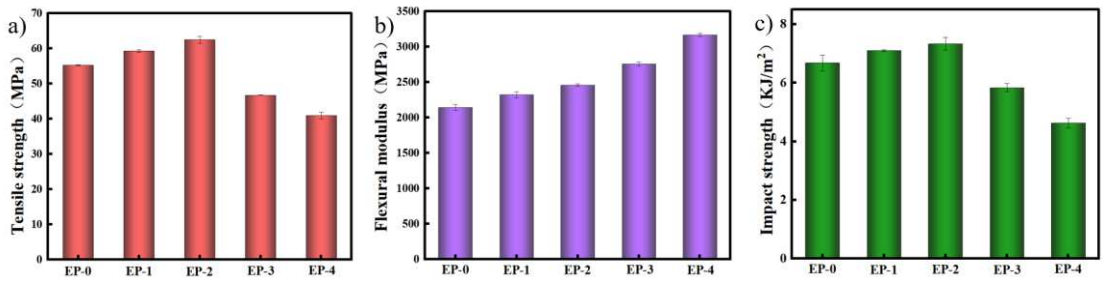


Fig. 10 Mechanical property analysis of epoxy resin composites a) Tensile strength b) Bending modulus c) Impact strength

Fig. 10 presents the mechanical properties of epoxy resin composites. After the addition of [ChlMIM][H_2PO_2], the tensile strength and impact strength of epoxy resin show a trend of first increasing and then decreasing with the rising dosage, and both reach their maximum values at EP-2, with a tensile strength of 62.66 MPa and an impact strength of 7.23 kJ/m^2. The flexural modulus exhibited a continuous upward trend. Tensile strength, impact strength and flexural modulus correspond to the mechanical responses of materials under different loading modes and serve as core indicators for evaluating their mechanical properties. Briefly speaking, tensile strength represents the material's ability to resist tensile fracture; flexural modulus stands for the rigidity against bending deformation; impact strength reflects the toughness to withstand instantaneous impact or collision.

Owing to its inherent chemical structural, [ChlMIM][H_2PO_2] can be incorporated into the crosslinked network of epoxy resin via curing reactions. Moreover, phosphorus, nitrogen and aromatic groups in its molecular structure can form chemical bonds or hydrogen bonds with epoxy groups, strengthening the intermolecular interaction forces[21-22]. Meanwhile, the flame-retardant acts as stress-dissipating sites to alleviate stress concentration under tension and impact, which account for the initial increase in tensile and impact strength. Nevertheless, agglomeration occurs when the dosage increases excessively. The weak interfacial bonding force between these agglomerates and the matrix leads to stress accumulation around agglomerates under tensile and impact loads, triggering interfacial debonding as well as crack initiation and

propagation, thereby deteriorating the mechanical performance of the material. In addition, excessive flame-retardant loading disrupted the continuity of the intrinsic crosslinked network within the epoxy resin matrix.

Flexural modulus characterizes material rigidity, and its steady growth originates from continuous rigidity enhancement. Regardless of the loading amount of flame-retardant, [ChlMIM][H_2PO_2] inherently possesses a rigid phosphorus-nitrogen heterocyclic structure, and phosphorus-containing components such as polyphosphoric acid are generated during heating. The proportion of such rigid structures increased with rising flame-retardant loading. Flexural loading refers to static bending that relies heavily on the rigid skeleton of materials. Therefore, even with internal agglomeration inside the material, the introduced rigid structures can still enhance the material's capacity to resist bending deformation, resulting in a sustained increase in flexural modulus[14-15].

3.9 Dynamic mechanical properties of EP-0 and EP-4

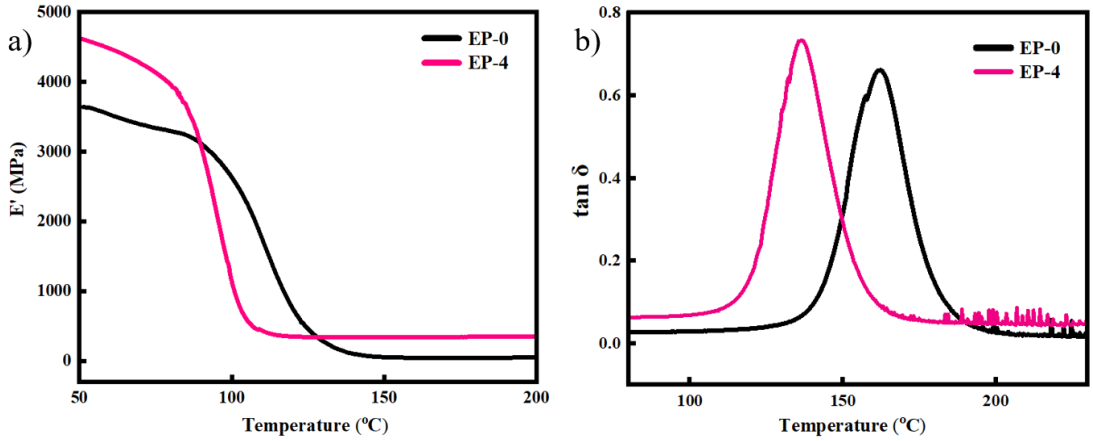


Fig. 11. Dynamic mechanical properties of EP-0 and EP-4: (a) storage modulus (E′) and (b) loss factor (tan δ).

As shown in Fig. 11 a), the incorporation of [ChlMIM][H_2PO_2] increased the storage modulus of the epoxy resin in both the glassy and rubbery regions. At approximately 50 °C, the storage modulus increased from about 3600 MPa for EP-0 to 4600 MPa for EP-4, indicating enhanced rigidity due to the rigid phosphorus–nitrogen structures and strong intermolecular interactions. Moreover, EP-4 exhibited a substantially higher rubbery plateau modulus, suggesting stronger effective network constraints. As shown

in Fig. 11 b), the tan δ peak shifted from approximately 162 °C for EP-0 to 137 °C for EP-4, indicating a decrease in the glass-transition temperature. This decrease may be attributed to the internal plasticization effect and increased local free volume introduced by the ionic liquid. Meanwhile, the higher and broader tan δ peak of EP-4 indicates enhanced damping capability and greater heterogeneity of the crosslinked network. Overall, [ChlMIM][H_2PO_2] enhanced the stiffness and high-temperature modulus of the epoxy resin while promoting segmental relaxation at a lower temperature.

4. Conclusion

In this work, the phosphorus/nitrogen-containing ionic liquid [ChlMIM][H_2PO_2] was successfully synthesized and introduced into DDM-cured E-51 epoxy resin to prepare flame-retardant epoxy composites. FTIR, ^{1}H NMR, and HRMS confirmed the chemical structure of [ChlMIM][H_2PO_2]. Owing to the synergistic effect of phosphorus and nitrogen, the ionic liquid markedly improved the fire safety of EP: the LOI value increased from 22.9% for EP-0 to 29.7% for EP-4, and the UL-94 rating improved from no rating to V-0. Compared with EP-0, EP-4 showed 30.4% and 29.8% reductions in THR and PHRR, respectively, while the char residue at 800 °C increased by 103.88%. TG-IR, SEM, and Raman analyses indicated that the enhanced flame retardancy resulted from condensed-phase and gas-phase synergism, in which phosphorus-containing species promoted the formation of a continuous and stable char layer, while nitrogen-containing components released inert gases to dilute flammable volatiles and suppress combustion. [ChlMIM][H_2PO_2] also improved the mechanical properties of EP. After adding [ChlMIM][H_2PO_2], the tensile strength of EP-4 is 40.185 MPa, the impact strength is 4.5454KJ/m^2, and the flexural modulus reaches 3150.4085MPa, representing a 46% improvement. The material exhibits favorable comprehensive properties. Overall, [ChlMIM][H_2PO_2] provides an effective strategy for preparing epoxy composites with enhanced flame retardancy and balanced mechanical performance.

Acknowledgements

This work was supported by the Basic Research Funds for Colleges and

Universities of Liaoning Province (No. LJ212410149019) and Shandong Provincial Innovation Capacity Enhancement Project for Science and Technology-Based Small and Medium-Sized Enterprises (No. 2025TSGC087).

Data Availability Statement

All data included in this study are available upon request by contact with the corresponding author.

Conflicts of interest

The authors declare that there are no conflicts to declare.

References

[1] Huo S, Song P, Yu B et al (2021) Phosphorus-containing flame retardant epoxy thermosets: Recent advances and future perspectives. Prog Polym Sci 114:101366. https://doi.org/10.1016/j.progpolymsci.2021.101366

[2] Zhi M, Yang X, Fan R et al (2022) A comprehensive review of reactive flame-retardant epoxy resin: Fundamentals, recent developments, and perspectives. Polym Degrad Stab 201:109976. https://doi.org/10.1016/j.polymdegradstab.2022.109976

[3] Jiang L, Liang B, Long JP (2024) Preparation of halogen-free flame retardant curing agent and its application in epoxy resin. High Perform Polym 36:508–518. https://doi.org/10.1177/09540083241280706

[4] Long JP, Liang B, Wang ZG (2020) Enhanced mechanical properties of APP flame-retardant epoxy resin by phosphorus-modified graphene oxide. Plast Rubber Compos 49:91–100. https://doi.org/10.1080/14658011.2019.1710067

[5] Kandola BK, Magnoni F, Ebdon JR (2022) Flame retardants for epoxy resins: Application-related challenges and solutions. J Vinyl Addit Technol 28:17–49. https://doi.org/10.1002/vnl.21890

[6] Varganici CD, Rosu L, Bifulco A et al (2022) Recent advances in flame retardant epoxy systems from reactive DOPO-based phosphorus additives. Polym Degrad Stab 202:110020. https://doi.org/10.1016/j.polymdegradstab.2022.110020

[7] Meng BW, Song MH, Liang B et al (2025) Synthesis of a new flame retardant and

performance study of flame retardant epoxy resin. High Perform Polym 37:32–39. https://doi.org/10.1177/09540083241302669

[8] Qiu YY, Liang B, Long JP (2025) Synthesis and application of novel imidazole-containing phosphorus–nitrogen flame retardants in epoxy resins. J Mater Sci 60:18136–18151. https://doi.org/10.1007/s10853-025-11526-w

[9] Wang D, Liu Q, Peng X et al (2021) High-efficiency phosphorus/nitrogen-containing flame retardant on epoxy resin. Polym Degrad Stab 187:109544. https://doi.org/10.1016/j.polymdegradstab.2021.109544

[10] Fang M, Qian J, Wang X et al (2021) Synthesis of a novel flame retardant containing phosphorus, nitrogen, and silicon and its application in epoxy resin. ACS Omega 6:7094–7105. https://doi.org/10.1021/acsomega.1c00076

[11] Zhang C, Duan H, Wan C et al (2022) Simultaneously improving the thermal stability, mechanical properties and flame retardancy of epoxy resin by a phosphorus/nitrogen/sulfur-containing reactive flame retardant. Mater Today Commun 30:103108. https://doi.org/10.1016/j.mtcomm.2021.103108

[12] Yang Y, Chen W, Li Z et al (2022) Efficient flame retardancy, good thermal stability, mechanical enhancement, and transparency of DOPO-conjugated structure compound on epoxy resin. Chem Eng J 450:138424. https://doi.org/10.1016/j.cej.2022.138424

[13] Huang Z, Wang S (2026) Recent progress of the preparation and application of superhydrophobic materials based on cotton fabric. J Appl Polym Sci 143(35):e71067. https://doi.org/10.1002/app.71067

[14] Ye G, Huo S, Wang C et al (2023) Durable flame-retardant, strong and tough epoxy resins with well-preserved thermal and optical properties via introducing a bio-based, phosphorus-phosphorus, hyperbranched oligomer. Polym Degrad Stab 207:110235. https://doi.org/10.1016/j.polymdegradstab.2022.110235

[15] Lou S, Wang S, Zhang L et al (2024) Intrinsic flame-retardant epoxy resin based on phosphorus-containing liquid imidazole compound: Simultaneously improving fire safety, mechanical property and heat resistance. Chem Eng J 493:152816. https://doi.org/10.1016/j.cej.2024.152816

[16] Pan K, Liu H, Wang Z et al (2023) Insights into ionic liquids for flame retardant: A study based on bibliometric mapping. Safety 9:49. https://doi.org/10.3390/safety9030049

[17] Shamsuri AA, Yusoff MZM, Abdan K et al (2023) Flammability properties of polymers and polymer composites combined with ionic liquids. e-Polymers 23:20230060. https://doi.org/10.1515/epoly-2023-0060

[18] Ou M, Lian R, Cui J et al (2023) Co-curing preparation of flame retardant and smoke-suppressive epoxy resin with a novel phosphorus-containing ionic liquid. Chemosphere 311:137061. https://doi.org/10.1016/j.chemosphere.2022.137061

[19] Wei L, Zhang X, Min F et al (2024) A flame-retardant and transparent epoxy resin based on phosphorus-containing ionic liquid and its mechanical, thermal and flame-retardant properties. React Funct Polym 197:105854. https://doi.org/10.1016/j.reactfunctpolym.2024.105854

[20] Xiao F, Shao W, Gao X et al (2024) A versatile ionic liquid enables epoxy resin with excellent fire safety and mechanical properties but ultra-low loading. Eur Polym J 219:113420. https://doi.org/10.1016/j.eurpolymj.2024.113420

[21] Zhang J, Liang J, Long J et al (2025) Synthesis of a novel DOPO-based ionic liquid flame retardant and its application in epoxy resin. J Mater Chem C 13:1844–1856. https://doi.org/10.1039/D4TC03681F

[22] Chen Y, Feng H, Li R et al (2025) A phosphorus-imidazole-based ionic liquid curing agent with high fire resistance and rapid curing capability, endowing epoxy resins with ultra-high toughness. Prog Org Coat 208:109522. https://doi.org/10.1016/j.porgcoat.2025.109522

[23] Yuan L, Yang Z, Zeng P et al (2024) Behavior and mechanism of flame retardant epoxy resins with intrinsic phosphorus-nitrogen phenolic resin curing agents. Eur Polym J 210:112959. https://doi.org/10.1016/j.eurpolymj.2024.112959

[24] Zhao Z, Yang Z, Shen W et al (2024) High fire-safety epoxy thermosets with a macromolecular phosphorus-nitrogen containing flame retardant at a low loading. Eur Polym J 215:113257. https://doi.org/10.1016/j.eurpolymj.2024.113257

[25] Wang H, Huo S, Wang C et al (2024) A P/N/Si-containing hyperbranched flame

retardant for improving mechanical performances, fire safety, and UV resistance of epoxy resins. Prog Org Coat 193:108562. https://doi.org/10.1016/j.porgcoat.2024.108562